Molecular Evolution of Ultraviolet Visual Opsins and Spectral Tuning of Photoreceptors in Anemonefishes (Amphiprioninae)

Laurie J. Mitchell [1,*], Karen L. Cheney [1], Martin Lührmann[2], Justin Marshall[2], Kyle Michie [2,3], and Fabio Cortesi [2,*]

[1]School of Biological Sciences, The University of Queensland, Brisbane, Queensland, Australia

[2]Queensland Brain Institute, The University of Queensland, Brisbane, Queensland, Australia

[3]King's College, Cambridge, United Kingdom

*Corresponding authors: E-mails: laurie.mitchell@uqconnect.edu.au; fabio.cortesi@uqconnect.edu.au.

Accepted: 5 August 2021

Abstract

Many animals including birds, reptiles, insects, and teleost fishes can see ultraviolet (UV) light (shorter than 400 nm), which has functional importance for foraging and communication. For coral reef fishes, shallow reef environments transmit a broad spectrum of light, rich in UV, driving the evolution of diverse spectral sensitivities. However, the identities and sites of the specific visual genes that underly vision in reef fishes remain elusive and are useful in determining how evolution has tuned vision to suit life on the reef. We investigated the visual systems of 11 anemonefish (Amphiprioninae) species, specifically probing for the molecular pathways that facilitate UV-sensitivity. Searching the genomes of anemonefishes, we identified a total of eight functional opsin genes from all five vertebrate visual opsin subfamilies. We found rare instances of teleost UV-sensitive *SWS1* opsin gene duplications that produced two functionally coding paralogs (*SWS1α* and *SWS1β*) and a pseudogene. We also found separate green sensitive *RH2A* opsin gene duplicates not yet reported in the family Pomacentridae. Transcriptome analysis revealed false clown anemonefish (*Amphiprion ocellaris*) expressed one rod opsin (*RH1*) and six cone opsins (*SWS1β, SWS2B, RH2B, RH2A-1, RH2A-2, LWS*) in the retina. Fluorescent in situ hybridization highlighted the (co-)expression of *SWS1β* with *SWS2B* in single cones, and either *RH2B*, *RH2A*, or *RH2A* together with *LWS* in different members of double cone photoreceptors (two single cones fused together). Our study provides the first in-depth characterization of visual opsin genes found in anemonefishes and provides a useful basis for the further study of UV-vision in reef fishes.

Key words: visual opsins, spectral tuning, reef fish vision, anemonefishes, ultraviolet, gene duplication.

Significance

Many coral reef fishes possess ultraviolet (UV) vision that is facilitated by UV-sensitive (*SWS1*) visual opsin proteins; however, the identities, sites, and evolution of *SWS1* genes are largely unknown and are important to understanding how reef fish vision has evolved to suit life on the reef. In the genomes of anemonefishes, we found eight functionally coding visual opsin genes, of which two were duplicate *SWS1* genes flanking a third pseudogenized copy, and one was expressed in the retina of anemonefish, *Amphiprion ocellaris*. Our findings provide new insights into the evolution of opsin gene diversity and spectral tuning of photoreceptors in an iconic group of reef fishes, particularly how gene duplication has produced multiple copies of *SWS1* potentially at and above the family level.

Introduction

Ultraviolet (UV) vision is widespread across the animal kingdom (Jacobs 1992; Tovée 1995) and is relied upon for many essential behaviors, including foraging (Church et al. 1998; Siitari et al. 2002; Boulcott and Braithwaite 2005; Novales Flamarique 2013), mate selection (Andersson and Amundsen 1997; Bennett et al. 1997; Smith et al. 2002; Rick and Bakker 2008a) and detecting potential competitors (Rick and Bakker 2008b; Siebeck et al. 2010; Bohórquez-Alonso et al. 2018). Underlying vision are the opsins, which are G-protein-coupled receptors with a Lysine residue (Lys296) that forms a Schiff base linkage to a carotenoid-derived (Vitamin A1 or A2) chromophore to form visual pigments mediating light absorbance from around 300 to 700 nm (Collin et al. 2009). UV-sensitivity is mediated by visual pigments with sensitivities shorter than 400 nm and is found in many vertebrates (Bowmaker 2008), including multiple teleost lineages (Lin et al. 2017; Musilova et al. 2019). Yet, for the majority of the approximately 30,000 teleost species we still lack detailed information on the identities, sites, and molecular evolution of specific genes and regulatory pathways that facilitate vision, including UV-sensitivity.

Visual opsins from all five vertebrate opsin subfamilies can be found in teleosts, including the UV-sensitive or very-short-wavelength-sensitive 1 (SWS1), short-wavelength-sensitive 2 (SWS2), medium-wavelength-sensitive, rhodopsin 1 (rod opsin, RH1) and rhodopsin-like 2 (RH2), and long-wavelength-sensitive (LWS) opsins (Yokoyama S and Yokoyama R 1996; reviewed by Carleton et al. 2020; Musilova et al. 2021). All of these families arose from an ancient vertebrate opsin that underwent multiple whole-genome and individual gene duplication events (Van de Peer et al. 2009), the latter of which facilitated the acquisition of novel visual opsin copies in multiple teleost lineages (Chinen et al. 2003; Matsumoto et al. 2006; Hofmann and Carleton 2009; Rennison et al. 2012; Musilova et al. 2019; Escobar-Camacho et al. 2020). Further changes to the available opsin gene repertoire can include their preservation and/or resurrection via gene conversion, a homogenizer of paralogous genes (Katju and Bergthorsson 2010; Cortesi et al. 2015), whereas modifications to opsin gene function mostly occur via amino acid substitutions (i.e., mutation) at "key-tuning sites" that determine the wavelength of maximum absorption (λ_{max}) sensitivity (Yokoyama 2000). Currently most of what is known on teleost opsin gene evolution pertains to the *SWS2, RH1*, *RH2*, and *LWS* subfamilies for which functional paralogs have been described (Chinen et al. 2005; Rennison et al. 2012; Cortesi et al. 2015), whereas the duplication and retention of *SWS1* paralogs are rare (Rennison et al. 2012; Lin et al. 2017; Musilova et al. 2019).

Teleost retinas contain both single and double cone (i.e., two-fused single cones that may be optically coupled) photoreceptors, the former of which expresses *SWS1* and/or *SWS2* opsin to convey UV and violet/blue sensitivity, respectively (Dalton et al. 2017; Stieb et al. 2019), whereas sensitivity to longer wavelengths is conveyed by the expression of *RH2* and/or *LWS* in double cones (Carleton et al. 2005, 2008; Parry et al. 2005; Spady et al. 2006; Dalton et al. 2015). It is changes in the opsin protein that drive most of the variation in visual pigment spectral tuning (Nickle and Robinson 2007; Carleton et al. 2020), particularly in the UV-region (~360–400 nm) (Yokoyama et al. 2016). Changes in the polarity and/or charge of amino acid residues at sites near the binding pocket can induce a short- or long-wavelength shift in spectral sensitivity (Carleton et al. 2005; Terai et al. 2006; Carleton 2009). The cumulative tuning effects of these sites may be used to estimate the peak spectral absorbance of visual pigments (Yokoyama et al. 2008), including SWS1-based pigments (Shi and Yokoyama 2003; Yokoyama et al. 2016). Further alterations to the spectral tuning of vision can be achieved by differential opsin expression (Fuller et al. 2004; Johnson et al. 2013; Cortesi et al. 2016; Shimmura et al. 2017) and/or coexpression of opsins in the retina (Dalton et al. 2014, 2017; Cortesi et al. 2015, 2016; Luehrmann et al. 2019; Stieb et al. 2019), which can adjust to match changes in light environment such as with depth, turbidity, and diet (Fuller and Claricoates 2011; Novales Flamarique 2013; Dalton et al. 2015; Stieb et al. 2016).

In shallow environments, such as coral reefs, which are rich in UV-wavelengths, small-bodied teleost fishes often possess *SWS1* opsin genes expressed in single cones (Phillips et al. 2016; Stieb et al. 2016, 2017, 2019) and have UV-transmissive lenses (Siebeck and Marshall 2001, 2007; Losey et al. 2003). UV-vision in reef fishes is thought to aid the detection of UV-reflecting zooplankton prey (Stieb et al. 2017) and/or facilitate a short-distance communication channel hidden from predators, most of which lack UV-sensitive photoreceptors (Losey et al. 1999; Marshall et al. 2006; Siebeck et al. 2010). However, despite the widespread nature of UV-sensitivity and its importance in reef fishes, its genetic basis remains largely uncharacterized, which we aimed to address in this study.

To do this, we used anemonefishes [family, Pomacentridae (damselfishes); subfamily, Amphiprioninae], which are an iconic group of reef fishes that obligately associate with one or more species of sea anemone. They are also sequential hermaphrodites living in strict social hierarchies governed by body size; the largest fish is the female, the second largest is the male and all smaller fish are sexually immature subordinates (Buston 2003). Amphiprioninae is split into two broad clades (Rolland et al. 2018), from which the visual system of one species (*Amphiprion akindynos*) belonging to the major clade (25 spp.) has been previously characterized in detail (Stieb et al. 2019). However, little is known on the visual systems of other anemonefishes within this clade, nor species from the minor clade (3 spp.). *Amphiprion akindynos* possesses short-wavelength-sensitive single cones (~400 nm

λ_{max}) mostly expressing *SWS1* and a small area in the retina coexpressing *SWS1* with *SWS2B* opsins, and mid- to long-wavelength-sensitive double cones (498, 520, 541 nm λ_{max}) expressing *RH2B*, *RH2A*, and *LWS* opsins (Stieb et al. 2019). The spectral tuning of their photoreceptors may help to enhance the detection of zooplankton prey and/or enhance the chromatic contrast of their own UV-reflective skin patterns, which may benefit species recognition (Stieb et al. 2019). Whether UV-vision is of general importance to anemonefishes is unknown but characterizing visual opsin gene diversity and expression patterns in a wider range of species could begin to reveal the extent of its importance across Amphiprioninae.

The public availability of short- and long-read sequenced genomes for 11 species of anemonefishes has made it possible to study in detail the evolution of *SWS1* opsin genes in this group of reef fishes. We first identified the *SWS1* opsin genes and other visual opsin genes found in the genomes of anemonefishes and provided information from their synteny analysis and phylogenetic reconstruction. Second, we identified the visual transduction and shut-off pathway genes that regulate opsin activity to show their synteny in all examined species. Finally, we quantified opsin gene expression levels and observed spatial patterns of cone opsin expression using fluorescence in situ hybridization (FISH) in the retina of the false-clown anemonefish (*Amphiprion ocellaris*), which belongs to the minor clade and is therefore suitable for an interclade comparison with previously published data on *A. akindynos* (Stieb et al. 2019).

Results

Anemonefish Visual Opsin Genes: Identification, Phylogeny, and Synteny

Our *in silico* searches in the genomes of anemonefishes and *Pomacentrus moluccensis* yielded a total of eight fully coding opsin genes belonging to five opsin classes including one rod opsin *RH1*, two UV-sensitive *SWS1* opsins, a single violet-sensitive *SWS2* opsin, two to three blue-green-sensitive *RH2* opsins, and a single yellow-red-sensitive *LWS* opsin (fig. 1*A*; supplementary table 1, Supplementary Material online). All visual transduction pathway genes and shutoff genes present in other vertebrates/fish species were also identified in *A. ocellaris* and Amphiprion *percula*, with no extra duplicates for these genes found (supplementary table 2, Supplementary Material online).

Two UV-sensitive opsins, *SWS1α* and *SWS1β*, were identified in all examined anemonefishes. Those found in *A. percula* and *A. ocellaris*, matched the sequence predictions on Ensembl (Ensembl transcript ID: ENSAOCT00000030401.1, ENSAOCT00000007343.1, ENSAPET00000035041.1, ENSAPET00000035052.1). The *A. percula* genome showed that both *SWS1* genes were located in-tandem on Chromosome 21, separated by 19 kb and spanning a total syntenic region of 29 kb. A third, nonfunctional *SWS1* pseudogene was also found in all anemonefishes (fig. 1*A*) that in the *A. percula* genome was situated between *SWS1α* and *SWS1β* (fig. 1*B*). *SWS1* pseudogenes in *Amphiprion sebae*, *Amphiprion bicinctus*, *Amphiprion nigripes*, *Amphiprion melanopus*, *Amphiprion akallopisos*, and *Amphiprion frenatus* had highest sequence homology to the initial two exons of *SWS1α*, whereas those in *A. ocellaris*, *A. percula*, *Amphiprion biaculeatus*, *Amphiprion polymnus*, and *Amphiprion perideraion* were most similar to *SWS1β*. The intronic region beyond Exon 2 of the *SWS1* pseudogene continued for approximately 300 bp, after which it substantially differed from equivalent regions in *SWS1α* and *SWS1β*, with no further detectable exons. *SWS1* pseudogenes in *A. ocellaris*, *A. akallopisos*, *A. bicinctus*, and *A. biaculeatus* were found to have premature stop codons at various amino acid sites, and in *A. ocellaris* a missense mutation caused by a single guanine to cytosine substitution removed the start codon. The genes flanking the *SWS1* region (fig. 1*B*) in *A. percula* were identical to those in *A. ocellaris*. *SWS1* orthologs in anemonefishes ranged between 96.2% and 97.5% in similarity.

All anemonefishes were found to have at least two blue-green sensitive opsin genes; *RH2A* and *RH2B*, with the former having two duplicates: *RH2A-1* and *RH2A-2* detected in four of the species, including *A. percula*, *A. ocellaris*, *A. perideraion*, and *A. akallopisos* (fig. 1*A*). *RH2* opsin genes found in *A. percula* closely matched sequence predictions on Ensembl (Ensembl transcript ID: ENSAOCT00000002771.1, ENSAPET00000018561.1, ENSAOCT00000002796.1, ENSAPET00000018598.1, ENSAOCT00000002830.1, ENSAPET00000018632.1). Like in other examined teleosts (Lin et al. 2017), the *RH2* genes in *A. percula* (fig. 1*B*) and *A. ocellaris* were found in-tandem, spanning a region of approximately 29 kb and flanked by identical genes immediately up- and down-stream of the syntenic region. Orthologous *RH2A* genes were found to be highly conserved within pairs of sister-species, including: 1) *A. percula and A. ocellaris* (sharing *RH2A-1* = 99.6% and *RH2A-2* = 99.3% similarity), and 2) *A. akallopisos* and *A. perideraion* (sharing *RH2A-1* = 99.4% and *RH2A-2* = 99.1% similarity).

One violet-sensitive *SWS2B* opsin and red-sensitive *LWS* opsin were identified in all anemonefishes, and those in *A. percula* and *A. ocellaris* matched sequence predictions on Ensembl (Ensembl transcript ID: ENSAOCT00000024298.1, ENSAPET00000033644.1, ENSAOCT00000031935.1, ENSAPET00000033670.1). The chromosomal resolution of the *A. percula* genome revealed the locations of the *RH2 and SWS2B-LWS* syntenic regions (fig. 1*B*) in-tandem on Chromosome 6, separated by approximately 8.6 Mb; a conserved syntenic region shared by many other Percomorph species (Musilova et al. 2019).

Like most teleost fishes (Musilova et al. 2019), anemonefishes were found to possess a single *RH1* (fig. 1*A*), with a conserved *RH1* syntenic region (fig. 1*B*). Those found in *A.*

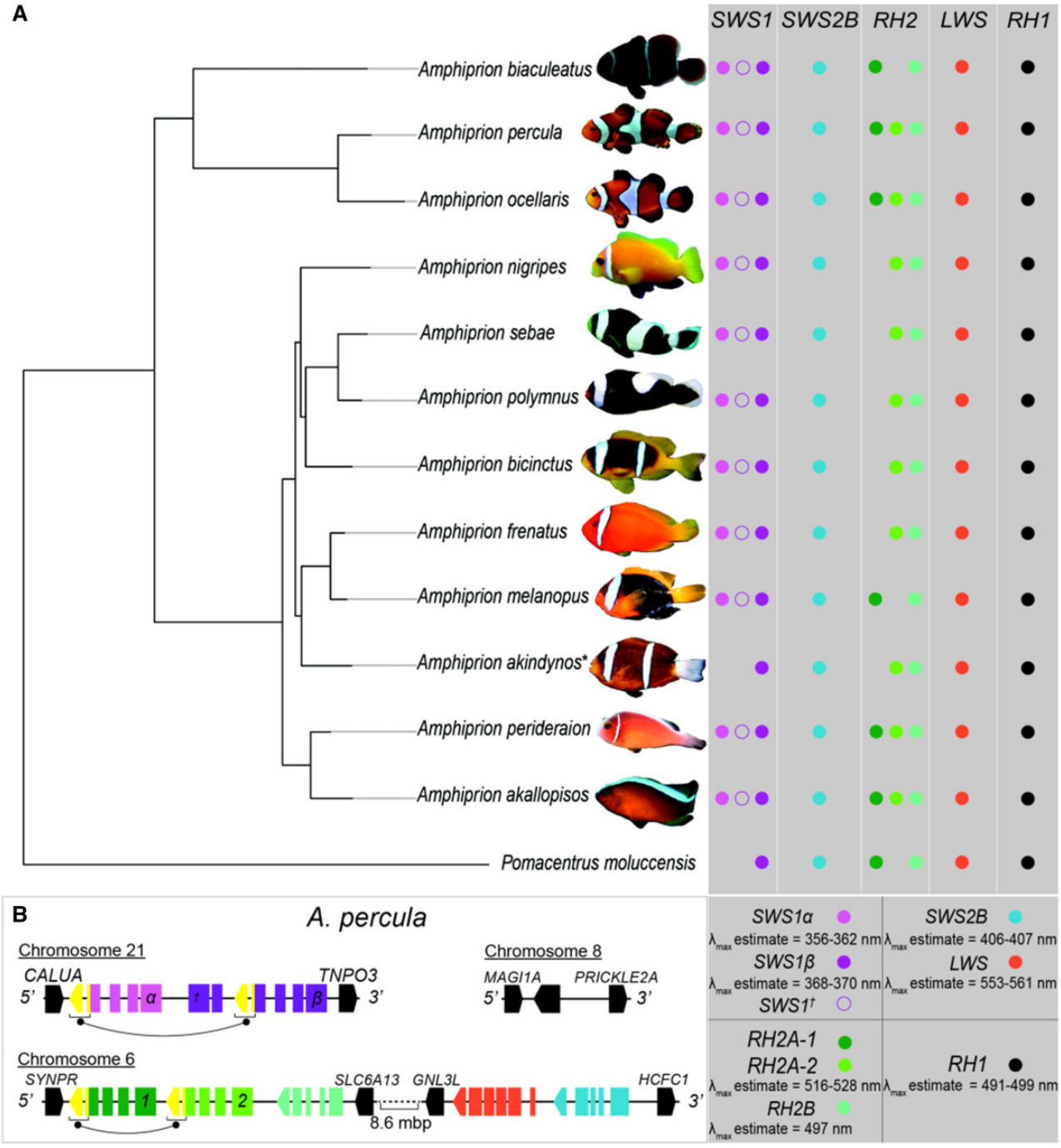

Fig. 1.—Summary of anemonefish visual opsin genes and their synteny. (*A*) Visual opsin genes mapped on the species tree (modified from Tang et al. [2021]) along with their range of estimated peak spectral absorbance (λ_{max}) values. A detailed opsin gene phylogeny is presented in supplementary figure 2, Supplementary Material online. (*B*) Synteny of anemonefish visual genes according to the chromosomal arrangement in *Amphiprion percula*, including opsin gene coding regions (boxes depict single exons) and their flanking genes (black). Areas highlighted in yellow indicate regions where recombination occurred between opsin gene paralogs. Opsin gene acronyms stand for: *RH1*, rhodopsin 1 (rod opsin); *RH2*, rhodopsin-like 2; *SWS2*, short-wavelength-sensitive 2; *LWS*, long-wavelength-sensitive; *SWS1*†, short-wavelength-sensitive 1/short-wavelength-sensitive pseudogene. *Opsin genes mapped from raw transcriptome reads of the *A. akindynos* retina (from Stieb et al. [2019]). Image credit: *A. nigripes*, Ewa Barska via Wikimedia Commons; *A. polymnus*, Jens Petersen via Wikimedia Commons; *A. bicinctus*, Patryk Krzyzak via Wikimedia Commons; *A. frenatus*, Vincent Chen via Wikimedia Commons; *A. ocellaris* and *A. akindynos*, Valerio Tettamanti via direct permission.

ocellaris and A. percula genomes matched predicted sequences on Ensembl (Ensembl transcript ID: ENSAOCG00000018646, ENSAPEG00000012211).

Note that the *SWS1* pseudogene and *RH2A-2* paralog were first found in the highly resolved genomes of *A. percula* and *A. ocellaris* that were published by two independent lab groups that used different sequencing and assembly strategies (Tan et al. 2018; Lehmann et al. 2018) , making it unlikely that they are the product of assembly artefacts. Because the draft genomes of other anemonefishes are comparatively poorly resolved, the *SWS1* pseudogene, the full coding region of *SWS1α*, and *RH2A* paralogs where present, were extracted using the raw-read mapping approach in those cases. This incomplete or incorrect assembly of highly repetitive genomic regions is an inherent problem of short-read draft genomes (Richards 2018; Rice and Green 2019). To corroborate our results, we also used raw-read mapping on an independently sequenced short-read genome of *A. ocellaris* (bioproject: SRX5249785; Marcionetti et al. 2019).

Phylogenetic analyses placed all the identified opsin genes into distinct homologous clusters with their predicted opsin classes (supplementary fig. 2, Supplementary Material online). Furthermore, the translated and aligned protein sequences for the identified genes exhibited typical opsin traits including the conserved chromophore binding site residue (K296) and intact seven transmembrane domains. Phylogenetic analysis of *RH1*, *SWS2B*, *RH2B*, and *LWS* in anemonefishes (supplementary fig. 2, Supplementary Material online) showed a typical pattern of species-relatedness that mostly resembled the inferred phylogenies reported elsewhere (Tang et al. 2021). *RH2A and SWS1* phylogenies showed a clear separation of opsin gene paralogs, where *SWS1α* and *SWS1β* formed two clusters, and *RH2A-1* and *RH2A-2* formed two clusters (supplementary fig. 2, Supplementary Material online). Lone *RH2A* genes found in seven species mostly grouped with *RH2A-2* genes, with the exception of *A. melanopus* and *A. biaculeatus RH2A-1* genes.

Anemonefish Opsin Gene Conversion Analysis

We found evidence of gene conversion in both the *RH2A and SWS1* duplicates (fig. 1*B*). GARD analysis revealed three major breakpoints in the coding sequences of *RH2A-1* and *RH2A-2*. Alternative tree topologies based on the different *RH2A* breakpoint regions (supplementary fig. 3*A and B*, Supplementary Material online) supported recombination only at one located in Exons 4–5 (891–1,059 bp), as evident by a lack of orthologous clustering according to opsin gene that was recovered in trees based on a nonrecombined segment (1–890 bp), to reflect the phylogenetic relationships observed in the full opsin gene tree. Analysis of the aligned RH2A opsin protein sequences identified only one known key tuning site (aa site 292; site number given according to bovine rhodopsin) (Yokoyama and Jia 2020) located within the region of recombination.

Three breakpoints were also reported in the *SWS1α* and *SWS1β* duplicates. Alternative tree topologies supported the notion of gene conversion in one of these areas in Exons 4 and 5 (839–1,017 bp), where *SWS1* orthologs had partial clusters that differed from the clear separation observed in trees based on a nonrecombined segment (341–509 bp) and in the full opsin gene phylogeny. Analysis of the aligned SWS1 opsin protein sequences did not yield any known tuning site changes within the recombined region.

Analysis of Visual Opsin Tuning Sites and λ_{max} Value Estimation

Protein sequence analysis (table 1) revealed highly conserved SWS1 opsins that shared 95.0–96.2% similarity. Closer inspection of the protein sequences showed some of the differences between paralogs occurred at known SWS1 tuning sites (Shi and Yokoyama 2003; Yokoyama et al. 2008), and 90% were within the seven transmembrane domains. Two sites were found to have a nonpolar to polar shift including A118S and A114S (table 1), with the former known to induce a +5 nm shift in opsin λ_{max} (Shi and Yokoyama 2003) (see supplementary fig. 4, Supplementary Material online, for a comprehensive list of all variable aa sites). All SWS1 protein sequences had conserved F86 and S90 aa sites, an invariable feature of UV-sensitive opsins (Cowing et al. 2002). Estimated λ_{max} values for SWS1 opsins ranged from 356 to 362 nm for SWS1α, and 368 to 370 nm for SWS1β (fig. 1*A*). SWS1α and SWS1β opsin protein sequences were near-identical to those found in *Oryzias latipes* (λ_{max} value = 356 nm, Matsumoto et al. 2006) and *P. amboinensis* (λ_{max} value = 370 nm, Siebeck et al. 2010), respectively. Note, all λ_{max} values reported should be treated as rough estimates, as they do not consider the effect of potential unknown tuning sites and/or interactive tuning effects between sites. Therefore, physical absorption measurements will be necessary to verify our approach.

Multiple opsin protein tuning sites were identified in RH2B (table 1) and used to infer a single estimated λ_{max} value of 497 nm (fig. 1*A*). No separate estimates for the RH2A paralogs could be made due to a lack of differences in identifiable known tuning site effects between the copies. One variable amino acid site had a known tuning effect; F158L/I that causes a −10 nm shift (table 1), which was used to infer RH2A λ_{max} estimates = 516–523 nm for most species, and a slightly broader range in *A. nigripes*, *A. polymnus*, and *A. sebae* (estimated λ_{max} value = 516–528 nm) (fig. 1*A*). Other notable but unaccountable variable aa sites included Y37F and T266V, both of which consistently alternated state between RH2A paralogs (supplementary fig. 4, Supplementary Material online).

Two variable aa sites were found with known tuning effects in LWS opsins (table 1) and were used to give

Table 1
Details of Anemonefish Opsin Genes and Variable Amino Acid Sites with Known and Unknown Tuning Effects

	Opsins					
	SWS1α SWS1β	SWS2B	RH2B	RH2A-1 RH2A-2	LWS	RH1
Length (bp)	1,017	1,056	1,038	1,059	1,074	1,059
No. of amino acids	339	352	346	353	358	353
Variable aa sites with known tuning effects (±nm shift, aa position according to bovine rhodopsin)	A118S (+5)[a]	L46F (−6)[b] A109G (−2)[b] T118G (−15)[b] A164S (+6)[c] Y203F (+1)[d] W265Y (−15)[e]	M44I (+3)[f] Q122E (+15 to +17)[f] M207L (−7)[f]	F158L/I (−10)[g,h]	S164A (−7)[i] A164S (+6)[i]	D83N (−6)[j]
Variable aa sites with unknown tuning effects	F49C A125S	—	A41G S124A	Y37F T266V	—	A217T

[a]Shi and Yokoyama (2003).
[b]Yokoyama et al. (2007).
[c]Neitz et al. (1991).
[d]Carleton et al. (2005).
[e]Fasick et al. (1999).
[f]Yokoyama and Jia (2020).
[g]Parry et al. (2005).
[h]Spady et al. (2006).
[i]Yokoyama et al. (2008).
[j]Takahashi and Ebrey (2003).

estimated λ_{max} values = 560/561 nm in most species (fig. 1*A*), except for *A. nigripes*, *A. polymnus*, *A. sebae*, and *A. bicinctus* (estimated λ_{max} values = 553–561 nm). Anemonefish SWS2B opsin yielded six variable aa sites with known tuning effects (table 1) and were used to infer estimated λ_{max} values = 406/407 nm, which were consistent across anemonefishes.

RH1 opsin protein sequences were highly conserved across anemonefishes, with one variable aa site with a known tuning effect; D83N that causes a −6 nm shift. This was used to infer estimated λ_{max} values = 491–499 nm, which were consistent across anemonefishes.

Visual Gene Expression Analysis of *A. ocellaris*

Analyses of retinal transcriptomes revealed that under our aquarium lighting the *A. ocellaris* retina ($N = 4$) expressed one rod opsin, *RH1* (mean ± SD = 70.6 ± 11.5%), and six cone opsins including four double cone opsins: *RH2B* (35.3 ± 3.2%), *RH2A-1* (43.1 ± 6.7%), *RH2A-2* (10.1 ± 11.7%) and *LWS* (11.5 ± 6.8%), and two single cone opsins: *SWS1β* (59.1 ± 9.4%.) and *SWS2B* (40.8 ± 8.7%) (fig. 2). No trace of *SWS1α* expression was detected in three out of the four retinas, and only a small amount (1.5%) was detected in one retina. No apparent difference in opsin gene expression was found between males ($n = 2$) and females ($n = 2$) (fig. 2).

FISH of *A. ocellaris* Retina

Brightfield viewing of the retina revealed a regular square mosaic arrangement with a central single cone surrounded by four double cones (fig. 3*D*, *H*, and *L*). FISH analyses showed that short-wavelength-sensitive opsins, *SWS1β and SWS2B*, were mostly coexpressed in single cone photoreceptors (fig. 3*A–D*).

Medium- and longer-wavelength-sensitive opsins, *RH2B*, *RH2A*, and *LWS*, were exclusively expressed in double cone photoreceptors (fig. 3*E–L*). Among these, *RH2A* and *RH2B* were expressed throughout the retina in separate double cone members (fig. 3*E–H*).

LWS was expressed across the retina and only observed to be coexpressed with *RH2A* (fig. 3*I–L*). However, although *RH2A* and *RH2B* fluorescent signal strength varied little between different cells, *LWS* signal strength varied noticeably, suggesting that quantitatively *LWS* expression may have been more variable. In some double cone members, *RH2A* appeared to be the only expressed opsin, with little or no expressed *LWS* apparent judging by a very dim or nondetectable fluorescent signal.

Discussion

Visual Opsin Gene Diversity in Anemonefish Genomes

Anemonefish genomes revealed eight visual opsin orthologs belonging to all five ancestral vertebrate classes of opsin (Davies et al. 2012) including *SWS1*, *SWS2B*, *RH1*, *RH2A*, *RH2B*, and *LWS*, along with additional *SWS1 and RH2A* duplicates. We found instances of UV-sensitive *SWS1* opsin gene duplication events that produced two functional paralogs (*SWS1α* and *SWS1β*) and a pseudogene. The expressed

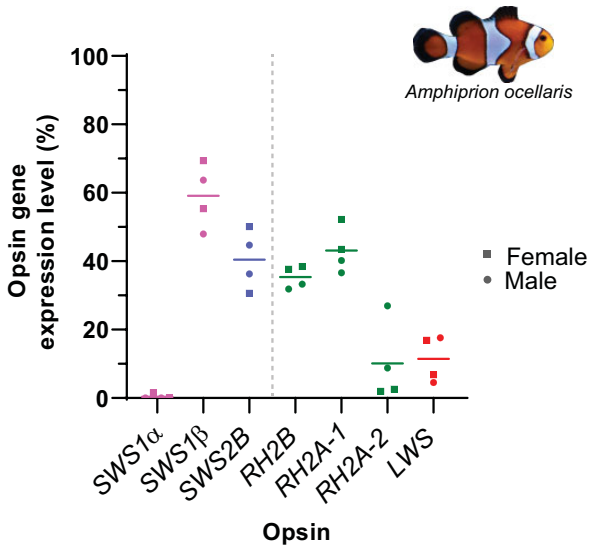

Fig. 2.—Relative cone opsin expression levels in the retina of captive *Amphiprion ocellaris* ($N = 4$; two females and two males) kept under aquarium lighting (see supplementary fig. 1, Supplementary Material online, for illumination spectra). Lines represent the mean proportion of opsin expression relative to the total opsin expression levels of single cones opsins (*SWS*s) and double cone opsins (*RH2*s, *LWS*), respectively. *SWS1*, short-wavelength-sensitive 1; *SWS2*, short-wavelength-sensitive 2; *RH2*, rhodopsin-like 2; *LWS*, long-wavelength-sensitive. Image credit: *Amphiprion ocellaris* via direct permission from Valerio Tettamanti.

cone opsin palette in the adult retina of *A. ocellaris* comprised *SWS1β* and *SWS2B* single cone opsins, in addition to *RH2A-1*, *RH2B*, and smaller amounts of *RH2A-2* and *LWS* in double cone opsin genes. No indication for the percomorph-specific *SWS2Aα* and *SWS2Aβ* was found, likely due to a double-gene loss in the damselfish ancestor (Cortesi et al. 2015).

Visual opsin genes found in the genomes of anemonefishes are situated in conserved regions that share a common synteny with other teleost fishes (Lin et al. 2017; Musilova et al. 2021). It also appears that anemonefish *SWS1* and *RH2* paralogs emerged through tandem duplication, as is common for opsin paralogs in many fish species (Cortesi et al. 2015; Lin et al. 2017; Musilova et al. 2019, 2021). It is extremely rare to find an *SWS1* opsin gene duplicate in teleosts (Rennison et al. 2012; Lin et al. 2017; Musilova et al. 2019, 2021). Here, we show that *SWS1* opsin duplicates are conserved across 11 members of Amphiprioninae but not present in a sister species *P. moluccensis* (subfamily Pomacentrinae), as similarly reported in the damselfish, *Stegastes partitus* (subfamily Microspathodontinae) (Musilova et al. 2019). Conversely, two *SWS1* opsin genes were reported in *Chromis chromis*; a member of the subfamily Chrominae (Musilova et al. 2019), and hence some Pomacentridae possess *SWS1* opsin duplicates. Thus, it remains unclear whether the gene duplication event that produced *SWS1α* and *SWS1β* was lineage- or subfamily-specific. More genomic data are needed to resolve whether this *SWS1* gene duplication occurred at the base of Pomacentridae or multiple times independently in its radiated lineages.

Interestingly, we found evidence of a second gene duplication event that produced a third, pseudogenized *SWS1* paralog in anemonefishes. The homology of this pseudogene was split roughly 50/50 between the *SWS1α* and *SWS1β* genes across anemonefish species with no clear phylogenetic pattern. This suggests the pseudogene either originated multiple times independently or more likely, because there is no clear phylogenetic pattern that subsequent gene conversion occurred after its duplication. The presence of this *SWS1* pseudogene across all examined members of both the minor and major anemonefish clades suggests that it emerged at the very least in the last common ancestor of both anemonefish clades.

Tuning of Anemonefish Single Cone Pigments and Potential Functional Significance

All SWS1α and SWS1β opsin protein sequences have conserved alanine at site 86 and serine at site 90, crucial for UV-sensitivity (Shi and Yokoyama 2003; Tada et al. 2009). Furthermore, both anemonefish SWS1 duplicates have intact open reading frames but only SWS1β is expressed at considerable levels in the adult retina. The (co)expression of SWS1β/SWS2B opsin genes in the single cones of *A. ocellaris* as revealed by FISH strongly implicates UV-vision mediated by SWS1 and SWS2B visual pigments in the single cones. Similarly, in *A. akindynos* SWS1 and SWS2B are coexpressed in some single cones (Stieb et al. 2019), although the amount of SWS2B was substantially lower (~10% of single cone opsin expression) than in *A. ocellaris* (~41%). This lower expression of SWS2B in *A. akindynos* is due to it being highly localized within a small, dorsotemporal (i.e., forward-looking) area in the retina of high acuity that may aid specific tasks such as foraging and intraspecific communication (Stieb et al. 2019). Whether any such spatial pattern in opsin expression exists in the *A. ocellaris* retina needs further investigation using detailed retinal topographic mapping of expressed cone opsin genes. We found no sex-related differences in opsin gene expression levels in *A. ocellaris*, an aspect shared by *A. akindynos* (Stieb et al. 2019). Because these two species are representatives from the two major anemonefish clades, it suggests that visual gene expression is independent of sex in these fishes.

The function of UV-vision in anemonefishes remains unclear but consideration of other UV-sensitive teleosts could provide important insights. Juvenile rainbow trout (*Oncorhynchus mykiss*) express *SWS1* opsin in their single cones that conveys UV-sensitivity to improve zooplanktivory efficacy by enhancing prey contrast (Novales Flamarique and

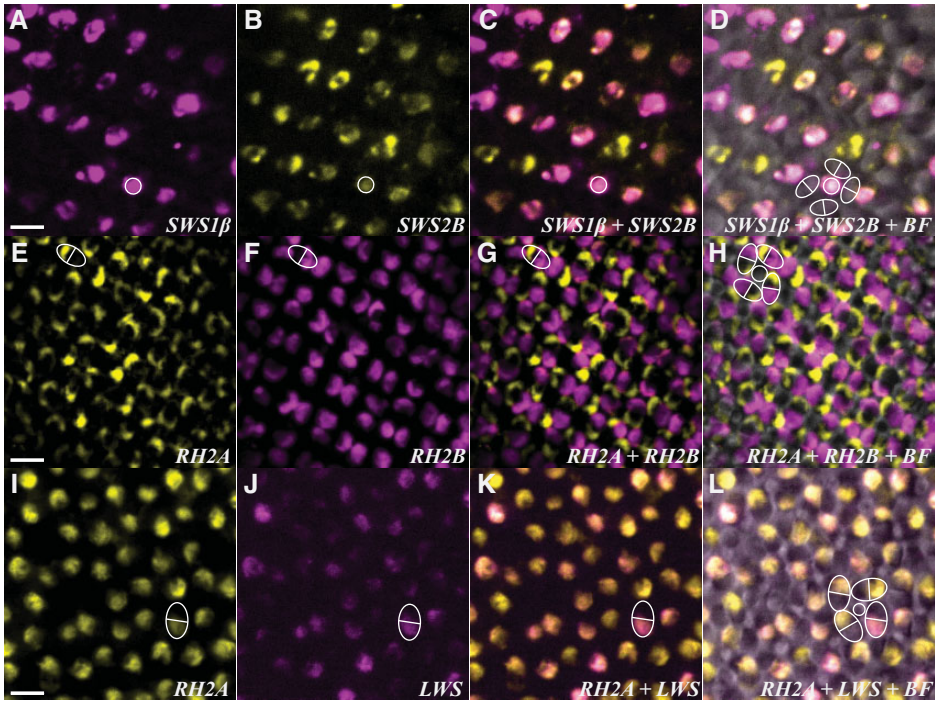

Fig. 3.—Double-labeling in situ hybridization of expressed opsin mRNAs in retinal single cone (*A–D*) and double cone (*E–L*) photoreceptors in adult *Amphiprion ocellaris*. (*A–D*) *SWS1β* (magenta) and *SWS2B* (yellow) mRNA were often coexpressed in the same single cones. (*E–H*) *RH2A* (yellow) and *RH2B* (magenta) mRNA were expressed in opposite members of double cones across the retina. (*I–L*) *RH2A* (yellow) and *LWS* (magenta) mRNA were expressed in the same double cone members. Representative single and double cones are outlines with a white circle and white ovals, respectively. BF, bright field. Scale bars = 10 μm.

Hawryshyn 1994; Novales Flamarique 2013). Similar foraging benefits conveyed by UV-sensitivity have been shown in perch (Loew et al. 1993), cichlids (Jordan et al. 2004), sticklebacks (Rick et al. 2012), and zebrafish (Novales Flamarique 2016; Yoshimatsu et al. 2020). Indeed, in damselfishes higher *SWS1* expression correlates strongly with zooplanktivory (Stieb et al. 2017), and anemonefishes are life-long zooplanktivores (Fautin and Allen 1997) that could similarly benefit from the enhanced UV contrast of prey in the water column.

Fish also use UV-signals for communicating with rivals and mates, as reported in the guppy (Smith et al. 2002), stickleback (Rick and Bakker 2008a, 2008b), and a damselfish (Siebeck et al. 2010). In *A. akindynos*, the coexpression of *SWS1* and *SWS2* is believed to increase the chromatic contrast of its skin color patterns that may improve the detection of conspecifics (Stieb et al. 2019). The use of UV-signaling in communication is worth further investigation in anemonefishes, as they possess UV-reflective skin patterns (Marshall et al. 2006; Stieb et al. 2019) that could conceivably be used to communicate their dominance status to other members within a family group and/or convey the occupied status of their hosted anemone to the members of rival groups from nearby anemones.

In principle, the advantages of UV-vision should be conveyable by a single UV-sensitive opsin, and the functional significance of possessing *SWS1* duplicates remains unknown. Another teleost species found to have two functionally coding *SWS1* duplicates is the smelt, *Plecoglossus altivelis* and like *A. ocellaris* it only expresses one paralog in adults (Minamoto and Shimizu 2005). As suggested in *P. altivelis*, it is possible that *SWS1α* is expressed in *A. ocellaris* during specific seasons such as winter months on the reef, when higher visibility from lower turbidity may promote the more efficient transmission of shorter wavelengths of light (Stieb et al. 2016). Similarly, increased *SWS1* opsin expression in the Nagasaki damsel, *P. nagasakiensis*, during winter has been suggested to be a visual tuning response for taking advantage of the higher UV (Stieb et al. 2016). Seasonal changes in opsin gene expression levels have been reported to alter color perception in widespread taxa (see review by Shimmura et al. [2018]).

Analyzing opsin expression levels in the larval and/or early-juvenile anemonefish retina may also reveal whether the shorter-wavelength-sensitive *SWS1α* is expressed during earlier life stages and whether an ontogenetic shift from *SWS1α* to *SWS1β* coincides with change(s) in light environment, particularly during the settlement stage when pelagic larvae return to the reef to seek a host anemone. Ontogenetic changes in cone opsin expression levels as a response to change in habitat have been reported in other reef fishes,

for example, spotted unicornfish (*Naso brevirostris*) (Tettamanti et al. 2019) and dusky dottyback (*Pseudochromis fuscus*) (Cortesi et al. 2016). Alternatively, the *SWS1α* opsin may be expressed in other tissues and/or organs, where animal opsins have been demonstrated to serve other sensory modalities, for example, nonimage forming vision, thermosensation, hearing (see review by Leung and Montell [2017]), taste (Leung et al. 2020), or potentially a nonsensory related function such as early eye and cranial development (see Novales Flamarique et al. 2021).

Tuning of Anemonefish Double Cone Pigments and Potential Functional Significance

The anemonefish double cones expressed a variety of opsins including two *RH2A* paralogs (*RH2A-1 and RH2A-2*), *RH2B and LWS*, almost all of which orthologs can be found in other pomacentrids (Hofmann et al. 2012; Stieb et al. 2016, 2017). However, to the best of our knowledge, this is the first report of an *RH2A* duplication in a pomacentrid. Similar *RH2A* duplications have been reported in most percomorphs (as reviewed by Musilova et al. [2019, 2021]). It was previously difficult to separate *RH2A* duplicates in pomacentrids due to their high degree of similarity, coupled with the low-resolution genomes available. Indeed, completely assembled *RH2A-2* genes could not be recovered in the draft genomes of *A. akallopisos* and *A. perideraion*, which were only detected by mapping against their raw paired-end genome reads. Neither approach recovered intact sets of duplicate *RH2A* opsin genes in 7 of the 11 anemonefishes likely due to gene loss, or alternatively due to incompleteness of genomic data.

The high level of similarity between detected *RH2A* orthologs was partly caused by gene conversion but could also be indicative of a fairly recent origin in the two clades of sister species (*A. ocellaris/A. percula* and *A. akallopisos/A. perideraion*). Regardless, it appears that *RH2A* genes are evolving quite dynamically in anemonefishes. Gene conversion at the fourth and fifth exons may act to preserve the opsin-chromophore binding site (Lys296), as is likely the case in *SWS1*. Additionally, the region of gene conversion in *RH2A* encompasses a known tuning site, bovine rhodopsin site number 292, where a large shift of −11 nm occurs when Ala is substituted with Ser (Yokoyama et al. 2007). Thus, preservation of this site by gene conversion may also have importance in preventing large shifts in the spectral tuning of RH2A visual pigments. RH2A regions lacking any detected gene conversion held a few variable amino acid sites between duplicates with unknown tuning effects. Some of these sites exhibited changes in polarity which may impact spectral tuning, particularly at sites Y37F and T266V whose identities alternated between paralogs. Subject to their exact tuning, the differential expression of RH2A opsins in the double cones may improve blue-green sensitivity, as has been suggested in cichlids to aid the viewing of nuptial skin colors and/or colonizing different depths (Weadick and Chang 2012; Dalton et al. 2014).

In the *A. ocellaris* retina, FISH indicated that *RH2A* opsin and *RH2B* opsin were always expressed in separate double cone members, whereas *LWS* was almost exclusively coexpressed with *RH2A*. One potential benefit of coexpressing *RH2A/LWS* is to increase light absorption and thus, enhance luminance contrast (Dalton et al. 2014). In African cichlids, the coexpression of *RH2A/LWS* is mostly limited to the ventral (i.e., upwards looking) retina, which likely aids the detection of distant dark objects such as predators against downwelling space light (Dalton et al. 2014). Whether a similar distribution of *LWS* is present in the *A. ocellaris* retina requires further investigation. Behavioural experiments involving fish reared under different light regimes (Fuller and Claricoates 2011; Dalton et al. 2015), or by taking a reverse genetic approach to assess the effect of specific opsin gene knockouts (Homma et al. 2017) could elucidate the function of opsin gene coexpression in anemonefishes.

Conclusions and Future Directions

Here we have shown that anemonefishes possess seven to eight visual opsin genes including duplications of the *SWS1* gene, and *RH2A* gene in some species. The presence of two functional *SWS1* opsins in all examined anemonefishes suggests a pomacentrid or at least anemonefish-specific *SWS1* gene duplication event, and a possibly lineage-specific second duplication event that produced an *SWS1* pseudogene. Moreover, most of these opsin genes were found expressed in the adult retinae of *A. ocellaris*. Our reported visual opsin gene expression levels and cone opsin mRNA labeling provide an initial glance at the opsin expression profile in the retina of captive *A. ocellaris*, and therefore, comparisons with wild anemonefish are required to assess differences associated with lighting, seasonality and/or ontogeny. Finally, we hope this information on the anemonefish visual system will encourage their use as a focus organism for investigating the mechanistic basis and function of UV-vision in reef fishes.

Materials and Methods

Anemonefish Visual Opsin Genes: Identification, Phylogeny, and Synteny

All genetic sequence analyses including the visual inspection, mapping, and alignment of genes were performed using Geneious Prime (v. 2019.2.1). Our in silico searches of anemonefish visual opsin genes involved annotating the regions containing the *SWS1*, *SWS2*, *RH2*, *LWS*, and *RH1* opsin genes, along with their immediate upstream and downstream (flanking) genes in the genomes of 11 species of anemonefish. The publicly available assembled genomes for anemonefishes were accessed from various sources including: *A. ocellaris* (Tan et al. 2018; accession number:

NXFZ00000000.1), *A. percula* (Lehmann et al. 2018; "Nemo Genome DB, 2018"; accession number: GCA_003047355.1), *A. frenatus* (Marcionetti et al. 2018; under bioproject: PRJNA433458), *A. akallopisos*, *A. melanopus*, *A. perideraion*, *A. nigripes*, *A. bicinctus*, *A. polymnus*, *A. sebae*, *A. biaculeatus*, and an outgroup sister species, the lemon damselfish, *P. moluccensis* (Marcionetti et al. 2019; under bioproject: PRJNA515163). Visual opsin genes were detected by mapping individual reference exon sequences from *Oreochromis niloticus* (accession numbers: AY775108, AF247128, JF262086, JF262087) and *Pseudochromis fuscus* (accession number: KP004335) using low specificity (>70% similarity) against anemonefish genomes. The full coding regions from duplicate *SWS1 and RH2A* opsin genes were detected in the high-quality long-read genome assemblies of *A. percula* (chromosome-resolution) and *A. ocellaris* (scaffold-resolution). However, only partially assembled opsin gene duplicates could initially be detected in the short-read genome assemblies of the other nine anemonefishes. Hence, to reconstruct the full coding sequences in those species we used a second approach that took advantage of the genomic raw-reads to back-map paired-end reads against the reference *A. percula*, *SWS1* and *RH2A* genes. This was followed by a "manual" approach that extracted highly similar gene duplicates by moving from one single-nuclear polymorphism (SNP) to another and taking advantage of paired-end information to breach gaps between SNPs (as per Musilova et al. [2019]). To complement our data set and further support opsin gene identity, we also remapped the transcriptomic reads from *A. akindynos* (accession number: SRX5993365; Stieb et al. 2019) against reference opsin gene sequences. Because that study did not specifically search for *SWS1* or *RH2* duplicates, we repeated the back-mapping approach using the transcriptomic raw reads in this case.

Visual transduction and shut-off pathway genes were also identified in the *A. percula* and *A. ocellaris* genomes by mapping against predicted gene sequences obtained from Ensembl v. 97 (ensembl.org, accession date: August 15, 2019) (Zerbino et al. 2018). The coding sequences were confirmed by mapping assembled transcripts from the *A. ocellaris* retina against the genes from Ensembl.

Phylogenetic trees based on the nucleotide alignment (MAFFT v. 7.388; Katoh and Standley 2013) of 135 visual opsin-coding sequences were generated using Bayesian inference in MrBayes v.3.2.7a (Huelsenbeck and Ronquist 2001) in a workflow run through CIPRES (Miller et al. 2012) and viewed using Figtree v. 1.4.4 (Rambaut 2018). We included *Anolis carolinensis* vertebrate ancestral opsin (accession number: NM_001293118) as an outgroup, and additional opsin sequences from distantly related species to show the grouping of anemonefish opsin genes relative to those found in other teleost fishes obtained from GenBank (www.ncbi.nlm.nih.gov/genbank/ last accessed August 18, 2021) including *Oreochromis niloticus* (AY775108, JF262088, JF262086, JF262087), *Pseudochromis fuscus* (accession numbers: KP004335, KP017247), *Danio rerio* (AB087811, HM367062, AB087803, NM_001002443, AF109369, KT008394, NM_182892, NM_131254, KT008398, KT008399), *O. latipes* (AB180742, XM_004069094, NM_001104694, AB223057, AB223058), and *Gasterosteus aculeatus* (KC774627, KC774623, KC594701, KC774625, KC774626). The opsin tree was reconstructed under a GTR+I+G model selected based on the best-fit model Akaike Information Criterion (AIC) from Jmodeltest2 (Darriba et al. 2012) with default parameters. The Bayesian reconstructions included MCMC searches for 10 million generations with two independent runs and four chains each, a sampling frequency of 1,000 generations and a burn-in of 25%.

Anemonefish Opsin Gene Conversion Analysis

Visual opsin gene duplicates were tested for gene conversion: a phenomenon commonly found in teleosts (Owens et al. 2009; Watson et al. 2011; Nakamura et al. 2013; Cortesi et al. 2015; Sandkam et al. 2017; Escobar-Camacho et al. 2017, 2020; Matsumoto et al. 2020). This was analyzed using the program GARD (Genetic Algorithm for Recombination Detection) (Kosakovsky Pond et al. 2006) on the aligned whole coding sequences of the *RH2A and SWS1* duplicates, respectively. Segments between reported breakpoint sites were identified as possible regions of recombination and corroborated by comparing different phylogenetic tree topologies based on those limited to suspected regions of recombination, and regions not suspected of recombination. Note that species with only a single *RH2A* gene were excluded from this analysis.

Analysis of Visual Opsin Tuning Sites and Λ_{max} Value Estimation

Comparisons between anemonefish opsin protein sequences and those of other fishes with known λ_{max} values were made to infer the spectral tuning effects of individual amino acid (aa) sites. Estimates of anemonefish opsin λ_{max} values were calculated from the known spectral absorbances of teleost opsins that have been thoroughly studied using either microspectrophotometry or direct measurement via in vitro reconstitution of opsin proteins including those found in *Oreochromis niloticus* and *Maylandia zebra* (Parry et al. 2005), *O. latipes* (Matsumoto et al. 2006), *Lucania goodei* (Fuller et al. 2003), *Pomacentrus amboinensis* (Siebeck et al. 2010), and *Dascyllus trimaculatus* (McFarland and Loew 1994). Our analysis involved identifying variable amino acid residues located at sites within the retinal binding pocket attributed to a shift in polarity and/or substitutions at previously reported tuning sites in those of other species. Opsin protein sequences were aligned using MAFFT alignment (MAFFT v.

7.388; Katoh and Standley 2013) with bovine (*Bos taurus*) rhodopsin as a template (PDB accession number: 1U19).

Animals and Ethics Statement

Anemonefish (*A. ocellaris*) ($N = 7$) (supplier Gallery Aquatica, Wynnum, QLD, Australia) used for opsin gene expression level analysis and FISH were housed in recirculating aquaria at the Queensland Brain Institute at the University of Queensland, Australia. Experiments were conducted in accordance with the University of Queensland's Animal Ethics Committee guidelines under the approval number: QBI/304/16.

Visual Gene Expression Analysis of *A. ocellaris*

Adult retinae from two female (mean standard-length = 45 mm) and two male (mean standard-length = 30 mm) *A. ocellaris* were sampled for opsin gene expression analysis. Teleost opsin gene expression levels can be highly plastic with detectable change occurring within as little as 1-month exposure to different lighting (Fuller and Claricoates 2011), and therefore, we kept fish under broad-spectrum lighting (supplementary fig. 1, Supplementary Material online) for a minimum of 3 weeks.

Isolated retinas were homogenized using a high-speed bench-top homogenizer and total RNA was extracted using the QiaGen RNeasy Mini Kit. RNA was purified from any possible DNA contamination by treating samples with DNase following the protocol outlined by the manufacturer (QiaGen). The integrity of the extract was subsequently determined using a Eukaryotic Total RNA Nanochip on an Agilent 2100 Bioanalyzer (Agilent Technologies). Total RNA was sent to Novogene (https://en.novogene.com/, last accessed August 18, 2021) for library preparation and strand-specific transcriptome sequencing on a Hiseq2500 (PE150, 250–300 bp insert). Retinal transcriptomes were then filtered and transcripts de novo assembled on a customised Galaxy (v2.4.0.2; usegalaxy.org) (Afgan et al. 2016) workflow following the protocol described in de Busserolles et al. (2017). Teleost single cone and double cone photoreceptors are morphologically and physiologically distinct entities, and proportional expression should be calculated separately between the two for a meaningful comparison (Yourick et al. 2019). Therefore, we calculated separate proportional cone opsin expression levels for *A. ocellaris* single and double cone genes. In brief, following de Busserolles *et al.* (2017), the number of mapped reads for each opsin gene was divided by its length (bp) and then normalized by the total number of reads mapped according to its cone type (i.e., against the combined single cone or double cone opsin gene expression).

A further step calculated separate proportional gene expression levels for *SWS1* and *RH2A* gene paralogs, by first extracting all the reads that mapped against both paralogs (e.g., *SWS1α* and *SWS1β*) and remapping them against a highly heterozygous region (i.e., a region with a high number of SNPs) of the paralogous pairs, including 341–509 bp (on the second exon) of *SWS1α* and *SWS1β*, and 633–892 bp (on the third and fourth exons) of *RH2A-1 and RH2A-2*. Individual expression levels for paralogs were then recalculated by multiplying the normalized number of remapped reads for each paralog by the initial proportion of the combined paralog expression (i.e., that was originally calculated using whole coding regions).

Rod versus cone opsin expression was calculated as the total proportion out of all mapped opsin reads.

FISH of *A. ocellaris* Cone Opsins

Dual-labeling FISH was performed on wholemount retinas from three adult *A. ocellaris*, following standard protocols (Raymond and Barthel 2004; Allison 2010; Dalton et al. 2014, 2015) using eyes that were enucleated and prepared following methods outlined by Barthel and Raymond (2000) after 1-h dark adaptation. Retinal mRNA was reverse transcribed using a High Capacity RNA-to-cDNA Reverse Transcription Kit (Applied Biosystems). Riboprobe templates were synthesized from cDNA via standard PCR using Q5 High Fidelity DNA polymerase (New England Biolabs) and opsin specific primers (supplementary table 1, Supplementary Material online). Amplicons were isolated via gel-electrophoresis and gel extraction (Qiagen Gel Extraction Kit), followed by enrichment PCR using gel-extracted amplicons as cDNA template. Primers were designed to bind to the coding sequence of target opsins (*LWS, RH2A, RH2B, SWS1β, SWS2B*) and to contain T3 or T7 RNA polymerase promoter sequences at their 5′-ends (T3, reverse primer; T7, forward primer) to allow subsequent strand-specific RNA transcription from cDNA templates for riboprobe synthesis. Because of the high similarity between RH2A paralogs, it was not possible to design riboprobes accurate enough to bind exclusively to either *RH2A-1* or *RH2A-2*. Antisense riboprobes were synthesized and labeled with digoxigenin-UTP (DIG) or fluorescein-UTP (FL) using DIG/FL RNA labeling mix (Roche). Hybridized, labeled riboprobes were detected using anti-digoxigenin or anti-fluorescein antibodies conjugated to horseradish peroxidase (Roche). Fluorescent tagging was performed using Alexa Fluor 594 or 488 dyes with streptavidin tyramide signal amplification (Invitrogen). Finally, retinas were mounted in 70% glycerol in PBS, photoreceptor side up, on microscopy slides with a coverslip.

Dual (*RH2A/RH2B, RH2A/LWS, SWS2B/SWS1β*) labeled photoreceptor cells were visualized and imaged at the Queensland Brain Institute's Advanced Microscopy Facility using a CFI Apo Lambda S LWD 40X/1.15 NA water immersion (*SWS1β/SWS2B, RH2A/RH2B*) and a CFI Apo Lambda 60×/1.4 NA oil immersion (*RH2A/LWS*) objective on a spinning disk confocal microscope (Diskovery, Andor Technologies, United Kingdom) built around a Nikon Ti-E body (Nikon Corporation, Japan) equipped with two Zyla 4.2 sCMOS cameras (Andor

Technology), and controlled by Nikon NIS Elements software (Nikon Corporation, Japan). Images were exported in TIFF file format and further processed with ImageJ (v.1.52p) (National Institute of Health, USA).

Supplementary Material

Supplementary data are available at *Genome Biology and Evolution* online.

Acknowledgments

We would like to thank Gillian Lawrence and the University of Queensland Biological Resources Aquatics Team for their support in maintaining aquaria, and Rumelo Amor from the Queensland Brain Institute's (QBI) Advanced Microscopy Facility for technical support. We also thank Karen L. Carleton, Sara Mae Stieb, and Daniel Escobar-Camacho for their insight and constructive feedback on the initial manuscript. This work was supported by an Australian Research Council Discovery Project (DP18012363) to J.M. and F.C., an Australian Research Council Future Fellowship (FT190100313) to K.L.C, an ARC DECRA (DE200100620) to F.C., and University of Queensland Development Fellowship to F.C.

Author Contributions

L.J.M., K.L.C., J.M., and F.C. conceived the study. L.J.M., K.M., and F.C. carried out gene identification and phylogenetic tree analyses. L.J.M. and F.C. conducted transcriptome analyses and calculated opsin gene expression levels. L.J.M. calculated estimates of visual pigment lambda max values. M.L. carried out FISH analyses. L.J.M wrote the initial draft manuscript, and all authors contributed to the final version.

Data Availability

Assembled transcriptomes underlying this article are available in Genbank, and can be accessed with (bioproject accession number: PRJNA547682). Opsin gene CDSs extracted from transcriptomes are also publicly available in GenBank (TPA accession numbers: BK059177—BK059184). Output files from phylogeny construction, GARD analyses, all genome and raw-read mapped opsin gene sequences, and DNA/protein alignments are available in the University of Queensland's Resource Data Manager platform, at (https://doi.org/10.14264/673b710, last accessed August 18, 2021).

Literature Cited

Afgan E, et al. 2016. The Galaxy platform for accessible, reproducible and collaborative biomedical analyses: 2016 update. Nucleic Acids Res. 44(W1):W3–W10.

Allison WT, et al. 2010. Ontogeny of cone photoreceptor mosaic in zebrafish. J Comp Neurol. 518(20):4182–4195.

Andersson S, Amundsen T. 1997. Ultraviolet colour vision and ornamentation in bluethroats. Proc R Soc Lond B Biol Sci. 264(1388):1587–1591.

Barthel LK, Raymond PA. 2000. In situ hybridization studies of retinal neurons. Methods Enzymol. 316:579–586.

Bennett ATD, Cuthill IC, Partridge JC, Lunau K. 1997. Ultraviolet plumage colors predict mate preferences in starlings. Proc Natl Acad Sci U S A. 94(16):8618–8621.

Bohórquez-Alonso ML, Mesa-Avila G, Suárez-Rancel M, Font E, Molina-Borja M. 2018. Predictors of contest outcome in males of two subspecies of *Gallotia galloti* (Squamata: Lacertidae). Behav Ecol Sociobiol. 72(3):1–11.

Boulcott P, Braithwaite V. 2005. Ultraviolet light and visual behaviour in the three-spined stickleback, *Gasterosteus aculeatus*. Physiol Biochem Zool. 78(5):736–743.

Bowmaker JK. 2008. Evolution of vertebrate visual pigments. Vision Res. 48(20):2022–2041.

Buston P. 2003. Size and growth modification in clownfish. Nature 424(6945):145–146.

Carleton K. 2009. Cichlid fish visual systems: mechanisms of spectral tuning. Integr Zool. 4(1):75–86.

Carleton KL, Escobar-Camacho D, Stieb SM, Cortesi F, Marshall NJ. 2020. Seeing the rainbow: mechanisms underlying spectral sensitivity in teleost fishes. J Exp Biol. 223(8):jeb193334.

Carleton KL, Parry JWL, Bowmaker JK, Hunt DM, Seehausen O. 2005. Colour vision and speciation in Lake Victoria cichlids of the genus *Pundamilia*. Mol Ecol. 14(14):4341–4353.

Carleton KL, et al. 2008. Visual sensitivities tuned by heterochronic shifts in opsin gene expression. BMC Biol. 6:22–14.

Chinen A, Hamaoka T, Yamada Y, Kawamura S. 2003. Gene duplication and spectral diversification of cone visual pigments of zebrafish. Genetics 163(2):663–675.

Chinen A, Matsumoto Y, Kawamura S. 2005. Reconstitution of ancestral green visual pigments of zebrafish and molecular mechanism of their spectral differentiation. Mol Biol Evol. 22(4):1001–1010.

Church SC, Bennett ATD, Cuthill IC, Partridge JC. 1998. Ultraviolet cues affect the foraging behaviour of blue tits. Proc R Soc Lond B Biol Sci. 265(1405):1509–1514.

Collin SP, Davies WL, Hart NS, Hunt DM. 2009. The evolution of early vertebrate photoreceptors. Philos Trans R Soc Lond B Biol Sci. 364(1531):2925–2940.

Cortesi F, et al. 2015. Ancestral duplications and highly dynamic opsin gene evolution in percomorph fishes. Proc Natl Acad Sci U S A. 112(5):1493–1498.

Cortesi F, et al. 2016. From crypsis to mimicry: changes in colour and the configuration of the visual system during ontogenetic habitat transitions in a coral reef fish. J Exp Biol. 219(Pt 16):2545–2558.

Cowing JA, et al. 2002. The molecular mechanism for the spectral shifts between vertebrate- ultraviolet- and violet-sensitive cone visual pigments. Biochem J. 367(1):129–135.

Dalton BE, de Busserolles F, Marshall NJ, Carleton KL. 2017. Retinal specialization through spatially varying cell densities and opsin coexpression in cichlid fish. J Exp Biol. 220:266–277.

Dalton BE, Loew ER, Cronin TW, Carleton KL. 2014. Spectral tuning by opsin coexpression in retinal regions that view different parts of the visual field. Proc R Soc Lond B Biol Sci. 281(1797):20141980.

Dalton BE, Lu J, Leips J, Cronin TW, Carleton KL. 2015. Variable light environments induce plastic spectral tuning by regional opsin coexpression in the African cichlid fish, *Metriaclima zebra*. Mol Ecol. 24(16):4193–4204.

Darriba D, Taboada GL, Doallo R, Posada D. 2012. JModelTest 2: more models, new heuristics and parallel computing. Nat Met. 9(8):772.

Davies WIL, Collin SP, Hunt DM. 2012. Molecular ecology and adaptation of visual photopigments in craniates. Mol Ecol. 21(13):3121–3158.
de Busserolles F, et al. 2017. Pushing the limits of photoreception in twilight conditions: the rod-like cone retina of the deep-sea pearlsides. Sci Adv. 3(11):eaao4709.
Escobar-Camacho D, Carleton KL, Narain DW, Pierotti MER. 2020. Visual pigment evolution in Characiformes: the dynamic interplay of teleost whole-genome duplication, surviving opsins and spectral tuning. Mol Ecol. 29(12):2234–2253.
Escobar-Camacho D, Ramos E, Martins C, Carleton KL. 2017. The opsin genes of amazonian cichlids. Mol Ecol. 26(5):1343–1356.
Fasick JI, Lee N, Oprian DD. 1999. Spectral tuning in the human blue cone pigment. Biochemistry 38(36):11593–11596.
Fautin DG, Allen GR. 1997. Anemonefishes and their host sea anemones: a guide for aquarists and divers. Perth: Western Australian Museum.
Fuller RC, Carleton KL, Fadool JM, Spady TC, Travis J. 2004. Population variation in opsin expression in the bluefin killifish, Lucania goodei: A real-time PCR study. J Comp Physiol A Neuroethol Sens Neural Behav Physiol. 190(2):147–154.
Fuller RC, Claricoates KM. 2011. Rapid light-induced shifts in opsin expression: finding new opsins, discerning mechanisms of change, and implications for visual sensitivity. Mol Ecol. 20(16):3321–3335.
Fuller RC, Fleishman LJ, Leal M, Travis J, Loew E. 2003. Intraspecific variation in retinal cone distribution in the bluefin killifish, *Lucania goodei*. J Comp Physiol A Neuroethol Sens Neural Behav Physiol. 189(8):609–616.
Hofmann CM, Carleton KL. 2009. Gene duplication and differential gene expression play an important role in the diversification of visual pigments in fish. Integr Comp Biol. 49(6):630–643.
Hofmann CM, et al. 2012. Opsin evolution in damselfish: convergence, reversal, and parallel evolution across tuning sites. J Mol Evol. 75(3–4):79–91.
Homma N, Harada Y, Uchikawa T, Kamei Y, Fukamachi S. 2017. Protanopia (red color-blindness) in medaka: a simple system for producing color-blind fish and testing their spectral sensitivity. BMC Genetics 18(1):10.
Huelsenbeck JP, Ronquist F. 2001. MRBAYES: Bayesian inference of phylogenetic trees. Bioinformatics 17(8):754–755.
Jacobs GH. 1992. Ultraviolet vision in vertebrates. Integr Comp Biol. 32:544–554.
Johnson AM, Stanis S, Fuller RC. 2013. Diurnal lighting patterns and habitat alter opsin expression and colour preferences in a killifish. Proc Biol Sci. 280(1763):20130796.
Jordan R, Howe D, Juanes F, Stauffer J, Loew E. 2004. Notes and records. Ultraviolet radiation enhances zooplanktivory rate in ultraviolet sensitive cichlids. Afr J Ecol. 42(3):228–231.
Katju V, Bergthorsson U. 2010. Genomic and population-level effects of gene conversion in *Caenorhabditis* paralogs. Genes 1(3):452–468.
Katoh K, Standley DM. 2013. MAFFT multiple sequence alignment software version 7: improvements in performance and usability. Mol Biol Evol. 30(4):772–780.
Kosakovsky Pond SL, Posada D, Gravenor MB, Woelk CH, Frost SDW. 2006. GARD: a genetic algorithm for recombination detection. Bioinformatics (Oxford, England). 22(24):3096–3098.
Lehmann R, et al. 2018. Finding Nemo's Genes: a chromosome-scale reference assembly of the genome of the orange clownfish *Amphiprion percula*. Mol Ecol Resour. 19(3):570–585.
Leung NY, Montell C. 2017. Unconventional roles of opsins. Annu Rev Cell Dev Biol. 33:241–264.
Leung NY, et al. 2020. Functions of opsins in *Drosophila* taste. Curr Biol. 30(8):1367–1379.e6.
Lin JJ, Wang FY, Li WH, Wang TY. 2017. The rises and falls of opsin genes in 59 ray-finned fish genomes and their implications for environmental adaptation. Sci Rep. 7(1):15568–15513.
Loew ER, McFarland WN, Mills EL, Hunter D. 1993. A chromatic action spectrum for planktonic predation by juvenile yellow perch, *Perca flavescens*. Can J Zool. 71(2):384–386.
Losey GS, et al. 1999. The UV visual world of fishes: a review. J Fish Biol. 54(5):921–943.
Losey GS, et al. 2003. Visual biology of Hawaiian coral reef fishes. I. Ocular transmission and visual pigments. Copeia 2003(3):433–454.
Luehrmann M, Carleton KL, Cortesi F, Cheney KL, Marshall NJ. 2019. Cardinalfishes (Apogonidae) show visual system adaptations typical of nocturnally and diurnally active fish. Mol Ecol. 28(12):3025–3041.
Marcionetti A, Rossier V, Bertrand JAM, Litsios G, Salamin N. 2018. First draft genome of an iconic clownfish species (*Amphiprion frenatus*). Mol Ecol Resour. 18(5):1092–1101.
Marcionetti A, et al. 2019. Insights into the genomics of clownfish adaptive radiation: genetic basis of the mutualism with sea anemones. Genome Biol Evol. 11(3):869–882.
Marshall J, Vorobyev M, Siebeck U. 2006. What does a reef fish see when sees a reef fish? In: Kapoor BG, Ladich F, Collin SP, editors. Communication in fishes. Enfield (NH): Science Publisher Inc. p. 393–422.
Matsumoto Y, Fukamachi S, Mitani H, Kawamura S. 2006. Functional characterisation of visual opsin repertoire in Medaka (*Oryzias latipes*). Gene 371(2):268–278.
Matsumoto Y, Oda S, Mitani H, Kawamura S. 2020. Orthologous divergence and paralogous anticonvergence in molecular evolution of triplicated green opsin genes in medaka fish, genus *Oryzias*. Genome Biol Evol. 12(6):911–923.
McFarland WN, Loew ER. 1994. Ultraviolet visual pigments in marine fishes of the family pomacentridae. Vision Res. 34(11):1393–1396.
Miller MA, Pfeiffer W, Schwartz T. 2012. The CIPRES science gateway: enabling high-impact science for phylogenetics researchers with limited resources. XSEDE '12: Proceedings of the 1st Conference of the Extreme Science and Engineering Discovery Environment: Bridging from the eXtreme to the campus and beyond. New York (NY): Association for Computing Machinery; 39:1–8. https://doi.org/10.1145/2335755.2335836.
Minamoto T, Shimizu I. 2005. Molecular cloning of cone opsin genes and their expression in the retina of a smelt, Ayu (*Plecoglossus altivelis*, Teleostei). Comp Biochem Physiol B Biochem Mol Biol. 140(2):197–205.
Musilova Z, Salzburger W, Cortesi F. 2021. The visual opsin gene repertoires of teleost fishes: evolution, ecology, and function. Annu Rev Cell Dev Biol. 37:21.1–21.28.
Musilova Z, et al. 2019. Vision using multiple distinct rod opsins in deep-sea fishes. Science 364(6440):588–592.
Nakamura Y, et al. 2013. Evolutionary changes of multiple visual pigment genes in the complete genome of Pacific bluefin tuna. Proc Natl Acad Sci U S A. 110(27):11061–11066.
Neitz M, Neitz J, Jacobs GH. 1991. Spectral tuning of pigments underlying red-green color vision. Science 252(5008):971–974.
Nickle B, Robinson PR. 2007. The opsins of the vertebrate retina: Insights from structural, biochemical, and evolutionary studies. Cell Mol Life Sci. 64(22):2917–2932.
Novales Flamarique H, Hawryshyn C. 1994. Ultraviolet photoreception contributes to prey search behaviour in two species of zooplanktivorous fishes. J Exp Biol. 186(1):187–198.
Novales Flamarique I. 2013. Opsin switch reveals function of the ultraviolet cone in fish foraging. Proc R Soc Lond B Biol Sci. 280(1752):20122490.
Novales Flamarique I. 2016. Diminished foraging performance of a mutant zebrafish with reduced population of ultraviolet cones. Proc R Soc Lond B Biol Sci. 283(1826):20160058.
Novales Flamarique I, et al. 2021. Disrupted eye and head development in rainbow trout with reduced ultraviolet (*sws1*) opsin expression. J Comp Neurol. 529(11):3013–3031.

Owens GL, Windsor DJ, Mui J, Taylor JS. 2009. A fish eye out of water: ten visual opsins in the four-eyed fish, *Anableps anableps*. PLoS One 4(6):e5970.
Parry JWL, et al. 2005. Mix and match color vision: tuning spectral sensitivity by differential opsin gene expression in Lake Malawi cichlids. Curr Biol. 15(19):1734–1739.
Phillips GAC, Carleton KL, Marshall NJ. 2016. Multiple Genetic Mechanisms Contribute to Visual Sensitivity Variation in the Labridae. Mol Biol Evol. 33(1):201–215.
Rambaut A. 2018. *FigTree, version 1.4.4*. Available from: http://tree.bio.ed.ac.uk/software/figtree/. Accessed August 18, 2021.
Raymond PA, Barthel LK. 2004. A moving wave patterns the cone photoreceptor mosaic array in the zebrafish retina. Int J Dev Biol. 48(8-9):935–945.
Rennison DJ, Owens GL, Taylor JS. 2012. Opsin gene duplication and divergence in ray-finned fish. Mol Phylogenet Evol. 62(3):986–1008.
Rice ES, Green RE. 2019. New approaches for genome assembly and scaffolding. Annu Rev Anim Biosci. 7:17–40.
Richards S. 2018. Full disclosure: genome assembly is still hard. PLoS Biol. 16(4):e2005894.
Rick IP, Bakker TCM. 2008a. UV wavelengths make female three-spined sticklebacks (*Gasterosteus aculeatus*) more attractive for males. Behav Ecol Sociobiol. 62(3):439–445.
Rick IP, Bakker TCM. 2008b. Males do not see only red: UV wavelengths and male territorial aggression in the three-spined stickleback (*Gasterosteus aculeatus*). Naturwissenschaften 95(7):631–638.
Rick IP, Bloemker D, Bakker TCM. 2012. Spectral composition and visual foraging in the three-spined stickleback (Gasterosteidae: *Gasterosteus aculeatus* L.): elucidating the role of ultraviolet wavelengths. Biol J Linn Soc. 105(2):359–368.
Rolland J, Silvestro D, Litsios G, Faye L, Salamin N. 2018. Clownfishes evolution below and above the species level. Proc R Soc B. 285(1873):1–9.
Sandkam BA, Joy JB, Watson CT, Breden F. 2017. Genomic environment impacts color vision evolution in a family with visually based sexual selection. Genome Biol Evol. 9(11):3100–3107.
Shi Y, Yokoyama S. 2003. Molecular analysis of the evolutionary significance of ultraviolet vision in vertebrates. Proc Natl Acad Sci U S A. 100(14):8308–8313.
Shimmura T, Nakayama T, Shinomiya A, Yoshimura T. 2018. Seasonal changes in color perception. Gen Comp Endocrinol. 260:171–174.
Shimmura T, et al. 2017. Dynamic plasticity in phototransduction regulates seasonal changes in color perception. Nat Commun. 8(1):412–417.
Siebeck UE, Marshall NJ. 2001. Ocular media transmission of coral reef fish—can coral reef fish see ultraviolet light? Vision Res. 41(2):133–149.
Siebeck UE, Marshall NJ. 2007. Potential ultraviolet vision in pre-settlement larvae and settled reef fish—a comparison across 23 families. Vision Res. 47(17):2337–2352.
Siebeck UE, Parker AN, Sprenger D, Mäthger LM, Wallis G. 2010. A species of reef fish that uses ultraviolet patterns for covert face recognition. Curr Biol. 20(5):407–410.
Siitari H, Viitala J, Hovi M. 2002. Behavioural evidence for ultraviolet vision in a tetraonid species—foraging experiment with black grouse *Tetrao tetrix*. J Avian Biol. 33(2):199–202.
Smith EJ, et al. 2002. Ultraviolet vision and mate choice in the guppy (*Poecilia reticulata*). Behav Ecol. 13(1):11–19.
Spady TC, et al. 2006. Evolution of the cichlid visual palette through ontogenetic subfunctionalization of the opsin gene arrays. Mol Biol Evol. 23(8):1538–1547.
Stieb SM, Carleton KL, Cortesi F, Marshall NJ, Salzburger W. 2016. Depth-dependent plasticity in opsin gene expression varies between damselfish (Pomacentridae) species. Mol Ecol. 25(15):3645–3661.
Stieb SM, et al. 2017. Why UV vision and red vision are important for damselfish (Pomacentridae): structural and expression variation in opsin genes. Mol Ecol. 26(5):1323–1342.
Stieb SM, et al. 2019. A detailed investigation of the visual system and visual ecology of the Barrier Reef anemonefish, *Amphiprion akindynos*. Sci Rep. 9(1):16459.
Tada T, Altuna A, Yokoyama S. 2009. Evolutionary replacement of UV vision by violet vision in fish. Proc Natl Acad Sci U S A. 106(41):17457–17462.
Takahashi Y, Ebrey TG. 2003. Molecular basis of spectral tuning in the newt short wavelength sensitive visual pigment. Biochemsitry 42(20):6025–6034.
Tan MH, et al. 2018. Finding Nemo: hybrid assembly with Oxford Nanopore and Illumina reads greatly improves the clownfish (*Amphiprion ocellaris*) genome assembly. Gigascience 7(3):1–6.
Tang KL, Stiassny MLJ, Mayden RL, Desalle R. 2021. Systematics of damselfishes. Ichthyol Herpetol. 109:258–318.
Terai Y, et al. 2006. Divergent selection on opsins drives incipient speciation in Lake Victoria cichlids. PLoS Biol. 4(12):e433.
Tettamanti V, de Busserolles F, Lecchini D, Marshall NJ, Cortesi F. 2019. Visual system development of the spotted unicornfish, *Naso brevirostris* (Acanthuridae). J Exp Biol. 222(24):jeb209916.
Tovée MJ. 1995. Ultra-violet photoreceptors in the animal kingdom: their distribution and function. Trends Ecol Evol. 10(11):455–460.
Van de Peer Y, Maere S, Meyer A. 2009. The evolutionary significance of ancient genome duplications. Nat Rev Genet. 10(10):725–732.
Watson CT, et al. 2011. Gene duplication and divergence of long wavelength-sensitive opsin genes in the Guppy, *Poecilia reticulata*. J Mol Evol. 72(2):240–252.
Weadick CJ, Chang BSW. 2012. Complex patterns of divergence among green-sensitive (RH2a) African cichlid opsins revealed by Clade model analyses. BMC Evol Biol. 12:206.
Yokoyama S. 2000. Molecular evolution of vertebrate visual pigments. Prog Retin Eye Res. 19(4):385–419.
Yokoyama S, Jia H. 2020. Origin and adaptation of green-sensitive (RH2) pigments in vertebrates. FEBS Open Bio. 10(5):873–882.
Yokoyama S, Tada T, Liu Y, Faggionato D, Altun A. 2016. A simple method for studying the molecular mechanisms of ultraviolet and violet reception in vertebrates. BMC Evol Biol. 16(1):64.
Yokoyama S, Tada T, Zhang H, Britt L. 2008. Elucidation of phenotypic adaptations: molecular analyses of dim-light vision proteins in vertebrates. Proc Natl Acad Sci U S A. 105(36):13480–13485.
Yokoyama S, Takenaka N, Blow N. 2007. A novel spectral tuning in the short wavelength-sensitive (SWS1 and SWS2) pigments of bluefin killifish (*Lucania goodei*). Gene 396(1):196–202.
Yokoyama S, Yokoyama R. 1996. Adaptive evolution of photoreceptors and visual pigments in vertebrates. Annu Rev Ecol Syst. 27(1):543–567.
Yoshimatsu T, Schröder C, Nevala NE, Berens P, Baden T. 2020. Fovea-like photoreceptor specializations underlie single UV cone rriven prey-capture behavior in zebrafish. Neuron 107(2):320–337.
Yourick MR, et al. 2019. Diurnal variation in opsin expression and common housekeeping genes necessitates comprehensive normalisation methods for quantitative real-time PCR analyses. Mol Ecol Resour. 19(6):1447–1460.
Zerbino DR. et al. 2018. Ensembl 2018. Nucleic Acids Res. 46(D1):D754–D761.

Associate editor: Takashi Makino